

BDC-based wind energy storage for multimode operating system

Vellarivelli B. Thurai Raaj^{1*}, Krishan Suresh¹, Ramasamy Arulmozhiyal²

¹ Department of EEE, VFSTR, Guntur 522213, AP, India

² Department of EEE, Sona Engineering College, Salem 636005, TN, India

Corresponding Author Email: info2vb@gmail.com

https://doi.org/10.18280/mmc_a.910305

Received: 2 August 2018

Accepted: 18 September 2018

Keywords:

Bidirectional Converter (BDC), main controller, inverter, wind energy, State of Charge (SOC)

ABSTRACT

We mainly focus on to creating a different mode of operation in an energy storage system for an effective way of wind energy utilization. The proposed energy storage system consists of Bidirectional DC–DC Converter (BDC), which makes the system effective in order to overcome the issues in practical usage. The modes of operations are based on three essential parameters such as wind-turbine speed (v), battery level (%) and load position (s). Based on the parameters' magnitude, the main controller will choose an effective mode. The main controller is designed in such a manner that it must be capable of withstanding drastic conditions, must be robust, should monitor all parameters, and could maintain the stability of the system. The work is evaluated through MATLAB/Simulink environment. Finally, the real time prototype experimental results are compared with that of the simulation. In addition, the proposed system is applicable for commercial and domestic power-storage systems.

1. INTRODUCTION

Nowadays, during summer season, the climate is subject to drastic change due to various reasons such as deforestation, urbanization, and the increase in the amount of pollutants (which is due to increase in the number of vehicles and industries). One of the reasons for this global warming is non-renewable form of power generation. Non-renewable forms of power generation are very harmful, which create acid rain and global warming. The available forms of renewable energy include wind, solar, tidal, biomass, and hydro-energy. Power plants that utilize these forms of energies leave no residue or slag and hence are said to be clean and eco-friendly. Electrical power equivalent of the available energy in the form of solar, wind, and hydro is 86000 TW, 870 TW, and 30TW, respectively, but the global demand is only 15TW. The major drawback in obtaining energy from these kinds of sources is the lesser efficiency of the energy-conversion devices. On the other hand, the global demand keeps on increasing, say at a rate of about 2% a year. Therefore, there should be some considerable increase in the rate of power generation, and that too from renewable forms of energy resources, since we must also consider environmental factors.

To extract constant power from windmill, several data samplings have been done in order to predict the availability of wind with respect to seasonal changes. Datum is estimated by the methods of random under-sampling and random over-sampling [1]. Here, power electronic grid emulator has been used under non-torque load conditions. Permanent magnet motor acts as the prime mover of the turbine. The net output has been connected to 10 kV grids. The test method is being divided into two groups: In first group, it tries to produce the output power up to 17MVA; in the second group, any grid fault that occurs will be identified with the help of smart sensors. A fuzzy adaptive droop control was employed to

control the multi terminal HVDC wind generation. It monitors the power capacity of wind turbine and coordinates between the voltage deviation and voltage sharing. It controls all other parameters based on the user's command. The fuzzy logic control never follows the mathematical procedure; instead, it follows the current data to find the best solution in an impulse manner [2-3].

The researcher proposed an optimal size of storage system for WPGM, based on charging and discharging of every storage system. Moreover, it adjusts the quantization index (QI) and finds out the fluctuation for various power-load conditions [4]. For finding out the accurate value, real time data are tested with previous three years' stored data. In the normal configuration, error has been measured and forecasted. Therefore, forecasting error has been neglected and the mean absolute error was taken into account [5]. Implementation of modified small signal as robust small signal stability for wind power generating scheme is proposed in this paper. Entire sector has been analyzed by 'state space model' to structure the parameters. The hyper plane approximation technique is followed to finalize those boundaries [6].

Stability mechanism and emergency control mechanism are integrated with wind power conversion system. Here, power electronics converters act as the main active power-controlling element. Due to their usage, rotor angle problem is being overcome and voltage stability is obtained. To further compensate/overcome the voltage instability, emergency Control method has been proposed [7]. Fuzzy logic proportional plus differential controller was proposed in permanent magnet synchronous generator based wind power generating scheme. Here, flywheel energy storage system has been integrated with wind turbine to regulate the frequency. Fuzzy PD controller proved to be the best suit under dynamic condition with the quickest response [8]. To ensure the reliability in wind power generating system, supervisory

control and data acquisition are used here to implement the hardware [9]. For wind power generation, orthogonal test support vector machine (OT-SVM) is proposed. It prevents the wind power plant from any unexpected failure. The real time testing was conducted at China with three various wind frames. OT-SVM helps to estimate the wind power availability while comparing other forecasting techniques [10]. Wind fluctuation plays a vital role in renewable energy, particularly in windmills. Storage of data in all aspects with respect to load demands is one of the way to predict the wind's availability in the future range [11].

In [12], Pulse frequency modulation (PFM) is proposed to improve the efficiency of converters. PWM based controllers are well equipped, but they have power loss in low power applications due to constant quiescent current. In order to overcome this, PFM technique based converter was developed, where series inductor controls the output voltage. Since load current is proportional to F_{sw} , efficiency is very high in light loads when compared to PWM technique. The major constraint is that the cost of this technique is higher than that of other solutions. A high-sensitive converter with high transient time response for that pseudo-wave tracking (PWT) is proposed. It has ensured safe and effective load changes from heavy load to light load and vice versa. It mainly focuses on the quick response applications like internet of things (IoT). Here, the current ripple is being sensed and is fed back to controller for corrective actions. The major drawback of this proposal is that during off-time it has fixed duration for both heavy load and light load conditions. Because of this constant time interval, power electronic switches are facing a reduction in their life-span [13].

Capacitor current sensor (CCS) based four-phase buck converter has been proposed for sensitive power applications. Initially, over shoot, under shoot, and settling time calculations have been estimated by theoretical assumption, and then CCS calibration determined the I_{co} at every instant. As per the calibration results, the four-phase control signals have updated them immediately, and therefore, transient response time of system had reduced [14]. Adaptive quasi-constant, on-time controller enables the fast transient response and it supports computer-integrated loads. Overall, the circuit has been designed based on a small signal model. The value of current in inductor determines the PWM value for switching. Inter-integrated circuit protocol is used as the communication channel between COTCM & AQCOTCM [15]. Dual buck

converter is proposed for analyzing the effects of stress in conductor switches. In addition, since it does not require any dead time, it remains unaffected by zero crossing distortion. As hardware, dsPACE with FPGA has been used to produce PWM; in this module, no feedback signal is used as a reference signal. The reference signals are directly sent to the modulator [16].

Implementation of an insulated alternative energy system and Zero voltage switching is preferred to change the sequence of current flow; totally four modes of operation were executed, each mode having forward ($\phi > \text{zero}$) and reverse ($\text{zero} < \phi$) power flow conditions. To achieve proper output, five inductors are used in this circuit, of which two act as a simple transformer while the rest are used in primary circuit. Super capacitor acts as a power reservoir at unexpected load condition [17-18]. A large-capacitance capacitor is used as a switching element, and to maintain the voltage gain in power circuit, two coupled inductors are introduced. Each and every buck and boost operation has two cycles: i.e., the first operating mode and the second operating mode, where both the modes of boost operation have their power flow in a direction opposite to that of their respective buck operation modes. The problem is that the life-span of the capacitor gets reduced due to overcharging [19]. Interleaved DC-DC Boost converter was also proposed in a renewable energy application, where the voltage stress across the switch affects its life-span [20]. Our proposed method overcomes those drawbacks and it provides uninterrupted power under various modes of operation.

2. PROPOSED METHOD

Natural wind energy is one of the affordable alternate renewable energy resources; it is the primary energy source for this proposed work. One of the disadvantages of wind energy is its reliability; it may be available or may not be (because of the environmental condition). The extraction of maximum possible power from wind energy with power electronics application is discussed in this paper. The proposed system is not wholly dependent on the renewable grid; here, the primary source is wind and the secondary source is battery, and if these two fail to provide energy, the system gets supply from the utility grid. It functions based on wind's availability, battery's level of charging and load position.

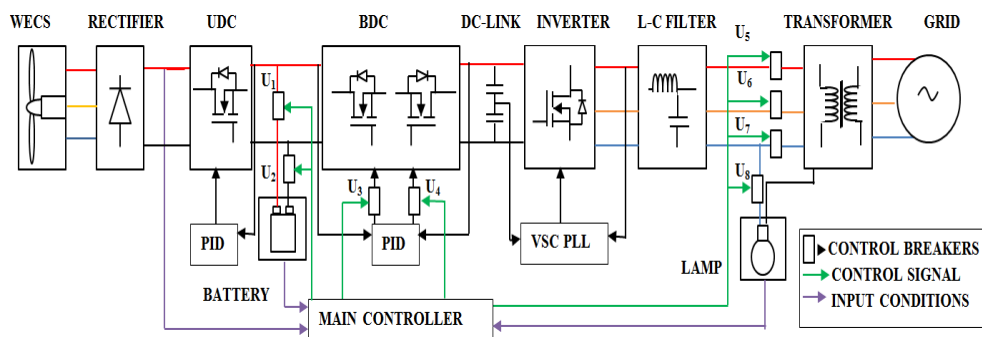


Figure 1. Block diagram of proposed system

This proposed system operates in five modes: The system's operation is designed for load in ON position and OFF position; therefore, it has been divided into nine modes. If the load is in

ON condition, the power from wind, battery and grid is supplied to the load; in this condition, the system operates in five modes and inverter operates in either stand-alone mode or

grid connected rectifier mode. On the contrary, when the load is in OFF condition, the generated power is exported to the grid; in this condition, the system operates in four modes and the inverter operates in grid-connected mode. The overall modes for ON position are, namely: wind power charging mode, wind power charging-output mode, wind power output mode, battery power load mode, and grid power charging-load mode. By using these five modes of operations, the proposed system acquires the available wind in an effective manner. During first four modes, BDC (Bidirectional DC-DC Converter) operates in boost mode, and during the fifth mode, it operates in buck mode. The proposed overall circuit diagram is as shown in figure 1.

3. MODES OF OPERATION

3.1 Wind powered battery mode (Mode-1)

The lay-out of wind powered battery mode can be explained with the help of block diagram, see figure 2. If the wind speed is greater than or equal to 5m/s, the Load switches itself to ON position; when the battery level is less than 40%, the control breakers U1 and U2 are forced to get closed and the battery goes to charging condition. The main control breaker supplies control signal to U1 and U2; only the remaining control breakers will be in OFF position. In this condition, the energy storage device is only allowed to charge; this mode continues until SOC level reaches greater than or equal to 40%. This mode is called wind-sourced battery mode. The circuit diagram of wind-powered battery mode is shown in figure 2.

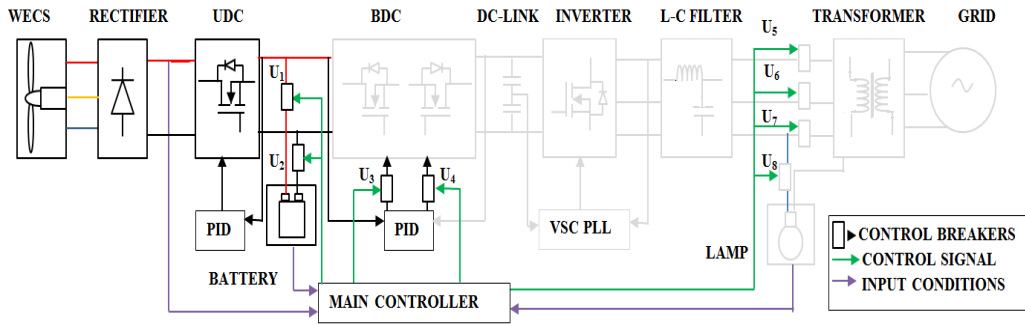


Figure 2. Wind powered battery mode

The wind power is converted into its electrical equivalent Eq(1); the coefficient of wind power is C_p .

$$P_e = \frac{1}{2} C_p (\beta, \lambda) \rho A u^3, \quad (1)$$

where ρ is the air density and u is the wind speed in m/s. [2] [3], [4] & [5] coefficient of power is given by

$$C_p = 0.22 \left(\frac{116}{\lambda_t} - 0.4\beta - 5 \right) e^{-\frac{12.5}{\lambda_t}} \quad (2)$$

Torque obtained from the wind turbine is given as

$$T_e = \frac{P_e}{\omega_m} \quad (3)$$

The output of PMSG is given in the following equations:

$$V_R = V_m \sin(\omega_0 t) \quad (4)$$

$$V_Y = V_m \sin\left(\omega_0 t - \frac{2\pi}{3}\right), \quad (5)$$

$$V_B = V_m \sin\left(\omega_0 t - \frac{4\pi}{3}\right) \quad (6)$$

where V_R , V_Y and V_B are the output voltages of PMSG. The rectifier output (V_r) is expressed in Eq. (7). From the above three Eqs., PMSG is given by

$$V_r = \frac{3V_m}{\pi} (1 + \cos\alpha) \quad (7)$$

The boost converter UDC's output (V_{bu}) is expressed as

$$V_{bu} = V_r \left(\frac{1}{1-D} \right) \quad (8)$$

The extracted charge of the battery is

$$Q_e = Q_{e_init} + \int -I_m(\tau) dt \quad (9)$$

where Q_e is the extracted charge (Ampere-second), Q_{e_init} is initial extracted charge (Ampere-second) and τ is integration time variable (time in second). The average current can be estimated by using the Eq.

$$I_{avg} = \frac{I_m}{(\tau_1 s + 1)}, \quad (10)$$

where I_{avg} is mean discharge current in Ampere, I_m = main branch current in Ampere and τ_1 = main branch time constant in seconds.

3.2 Wind power charging - output mode (mode-2)

Wind power charging-output mode has been explained with the help of block diagram as shown in figure 3. In this mode

of operation, the level of SOC is greater than or equal to 40% and lesser than 80%, the load is in ON position, and the wind speed is higher than or equal to 5m/s.

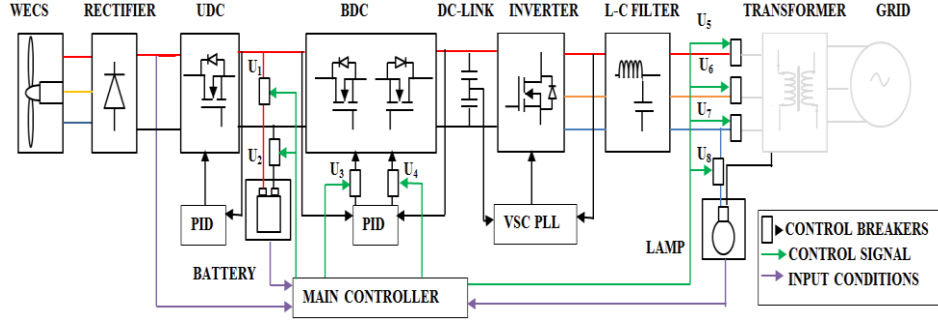


Figure 3. Wind power charging-output mode

The electrical energy obtained from Wind Energy Conversion System is fed to both battery and load. In this mode, input control breakers U1 and U2 allow charging of the battery and also the control breaker U3 allows supply to the load through bi-directional converter boost mode of operation. Based on the control breakers' operation, this process will be continued until the battery charge level becomes greater than or equal to 80%. This mode of operation is called wind power charging-output mode. The wind powered charging-output mode's circuit diagram is shown in Figure 3. The wind turbine power and rectifier to battery output Eqs. (1)-(10) in this mode are the same as in mode-1. The bidirectional converter's output Eq. (11) during boost mode is derived from unidirectional boost converter. In the line-to-output transfer-function, the open loop changes the output voltage due to a variation in the input voltage during the boost mode of BDC [8].

$$G_{id} = \frac{i_L}{d_{ab}} = V_{dc} \frac{1 + sZ_{ac}C_{ac}}{Z_{ac} + s^2L_{ac}Z_{ac}C_{ac}} \quad (12)$$

3.3 Wind power output mode (mode- 3)

Wind power output mode can be explained by the block diagram as shown in figure 4. The charging level of battery is greater than 80%, load is in ON position, and the wind speed is greater than or equal to 5m/s. The electrical energy obtained from Wind Energy Conversion System is given to either load or grid based on the load's manual position. In this mode, the input control breakers U1 and U2 get deactivated and they won't allow charging of the battery; therefore, control breaker U3 allows power from the supply to the load through bi-directional converter boost mode of operation. Based on the control breakers' operation, this process will be continued until the battery's SOC level gets reduced to less than 80%. The electrical energy from WECS is converted using converters via universal Bridge Rectifier, Unidirectional Converter, Bi-Directional converter (boost) and inverter in the boost mode. The final AC output is given to the load. This mode continues until the charging level is reduced to less than 80% or the wind speed is lower than 5 m/s. This mode of operation is called wind power output mode. The wind turbine power and rectifier to battery output Eqs. from (1) to (12) in this mode are the same as that in mode-1 and mode-2, except for battery charging.

$$\frac{\hat{V}_{batt}(s)}{\hat{V}_s(s)} = A_{gvf} \frac{1 + \frac{s}{\omega_s}}{1 + \frac{s}{\omega_L/C_1} + \frac{s^2}{\omega_L\omega_c/C_1}} \quad (11)$$

The three modes of buck rectifier/boost inverter units are standalone mode, grid-tied inverter mode, and grid-tied rectifier mode. These three modes are based on the wind energy electrical system's modes of operation. Stand-alone inverter mode is represented by

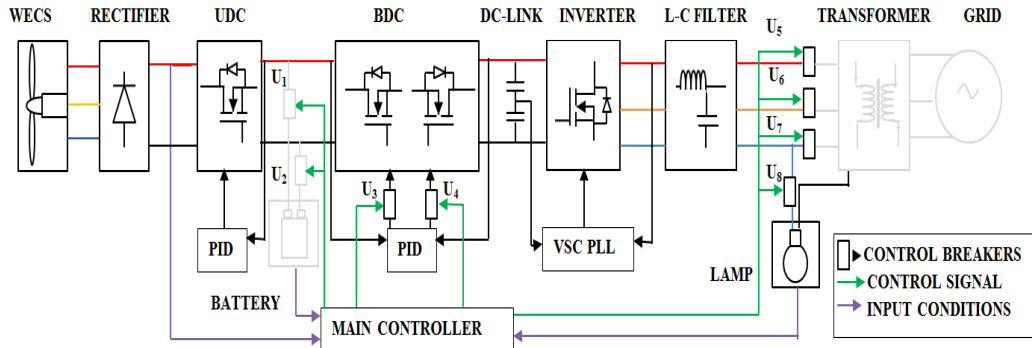


Figure 4. Wind power output mode

3.4 Battery power load mode (mode-4)

Battery power output mode can be explained by the block diagram as shown in figure 5. This mode takes place when the wind-speed W_m gets reduced below 5 meter/second, when load is in ON position or when the battery's state of charge is greater than or equal to 40%. Electrical energy obtained from wind energy is not in the range of required level. Hence, the battery output control breakers U_1 and U_2 turned to active position, and the bi-directional converter control breaker U_2

remains in active position and operates in boost mode. Hence, the battery supplies the electrical energy to the load. The battery output control breakers remain in an active condition until the level of battery's SOC reduced to 40% and wind speed reaches greater than or equal to 5 m/s. The wind turbine power and rectifier to battery output Eqs. from (9) to (12) in this mode are the same as that in mode-1 and mode-2, while the difference being the charging of the battery instead of discharging.

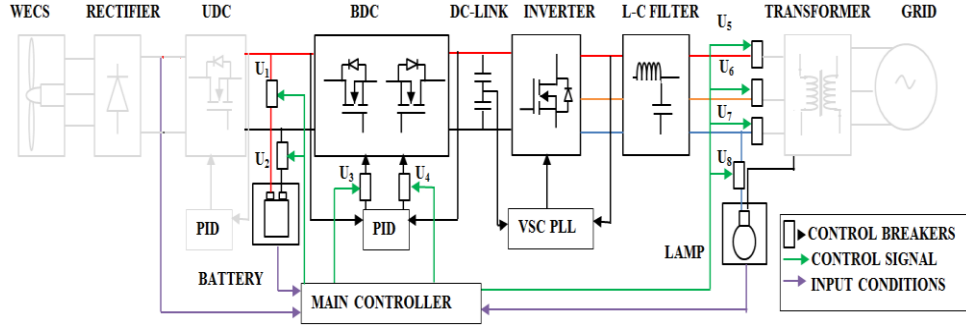


Figure 5. Battery power battery mode

3.5. Grid power battery-load mode (mode-5)

Grid power battery-load mode can be explained by the block diagram as shown in figure 6. In this mode, Bi-directional converter is operated in buck mode based on the switching of MOSFET's Q2 operations from high voltage side to low voltage side. Control breakers U_1 and U_2 of the battery's input and bi-directional converter U_4 (buck) are in active condition until the battery's SOC increases to greater than or equal to 80% or the wind speed reaches to greater than 5 m/s. Hence, the charging–discharging process continues in the buck and boost modes of operations. This mode of operation is called grid sourced battery mode. The grid output and PMSG output will be in three phase AC mode. Eqs. (4),

(5) and (7) give the output Eq. of grid, which is connected to the input of the inverter.

Grid-tied rectifier mode is represented by Eq. (13). The required condition for this mode is: wind speed less than 5 m/s, battery's state of charge less than 40% and the load in OFF condition. The grid supplies the power to the load and it charges the battery too. During this mode, the power should be drawn from the grid [11].

$$G_{id} = \frac{i_L}{d_{ab}} = V_{dc} \frac{2+sZ_{dc}C_{dc}}{d_{ab}^2 Z_{ac} + sL + s^2 L_{ac} Z_{dc} C_{dc}}, \quad (13)$$

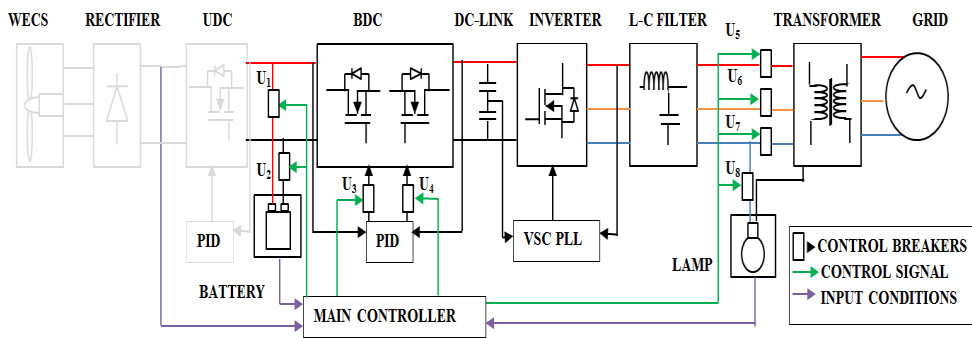


Figure 6. Grid power battery-load mode

The transfer function defines the compensator characteristics required in order to provide the overall open loop response to the system. In the line-to-output transfer function, the open loop change in the output voltage due to a variation in the input voltage is given by the following expression [8]:

$$\frac{\hat{v}_s(s)}{\hat{v}_{batt}(s)} = A_{gcf} \frac{1 + \frac{s}{\omega_{e1}}}{1 + \frac{s}{\omega_{Lcf}/C_b} + \frac{s^2}{\omega_{Lcf}\omega_{cfc}/C_b}} \quad (14)$$

The battery charging Eqs. (9) and (10) in this mode are the same as in mode-1 and mode-2 for charging.

4. SIMULATION AND REAL TIME RESULT COMPARISON

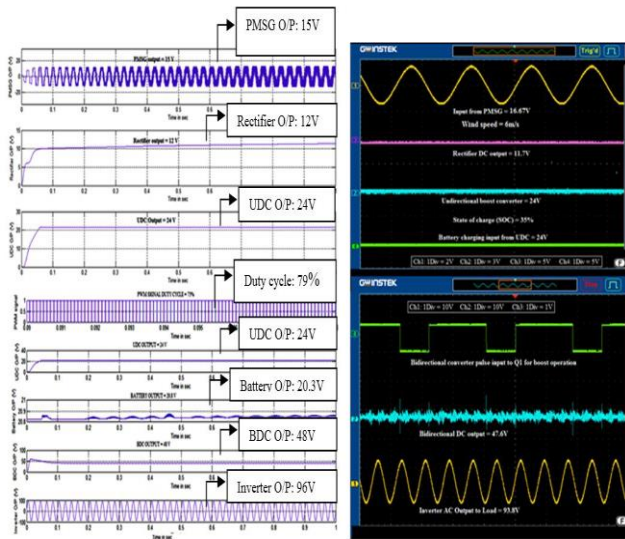


Figure 7. Output waveforms of mode-1, mode-2 and mode-3 when wind speed is at 6 m/s

The proposed system is simulated by MATLAB/Simulink environment, system is designed in hardware, and the results are compared with simulation results. The wind speed at less than 5 meters per second is used to reduce the wind profile parameters such as rotor speed and rotor torque. The PMSG is getting mechanical input from the wind turbine. When the wind speed is 3 meters per second, the output rotor torque is 0.7 N-m and the rotor speed is 37.7 radians per second. The PMSG’s output is 8.3V.

The wind profile consists of the analysis of wind speed, rotor speed, and rotor torque. The PMSG model is getting input from the turbine’s design. When the wind speed is 5

meters per second, the output rotor’s torque is 0.4 n-m and rotor speed is 76.7 radians per second. The PMSG’s output is 13.6V.

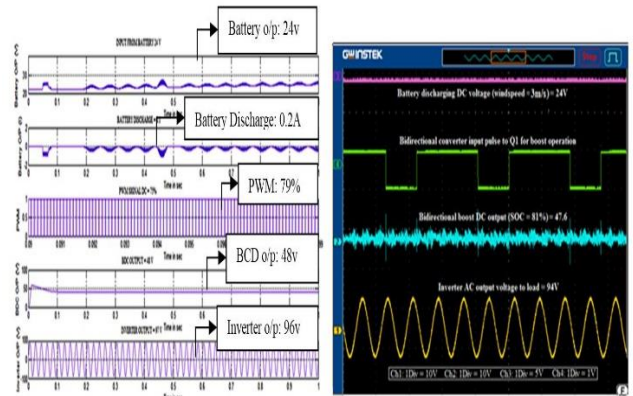


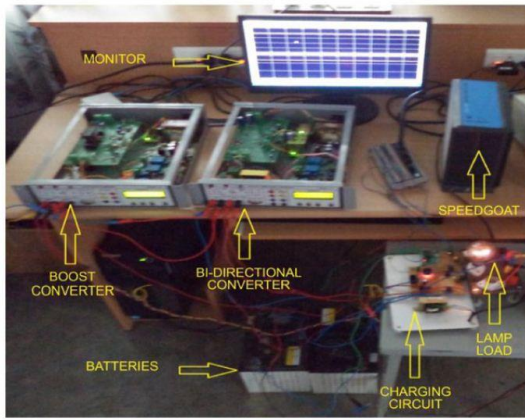
Figure 8. Output waveforms of mode-4 and mode-5 when wind speed is at 3 m/s

The experimental platform of overall system consists of a boost converter and bi-directional converter with PMSG. Figs. 9 -A & B show the hardware setup of bidirectional converter and storage systems and the real time experimental setup of wind mill. The performance of the unidirectional boost and bi-directional converter is being controlled by DSPIC30F4011 controller with PID control structure.

The resulting magnitudes of all the five modes are compared with simulation results. We found that the Real time output is almost equal to the simulation result. The system has a robust performance under changing input wind. The results of simulation and experiment are tabulated and compared. The experimental platform of overall system results is presented in Table 1. All the five modes’ results were obtained from different input wind-speeds. The real time output results are almost equal to the simulation results.

Table 1. Result of all the modes

Wind Energy Conversion		Energy Storage System Integrated with Grid									
Wind speed (m/s)	PMSG o/p (v)	Mode of operation	PMSG o/p (V)	Rectifier o/p (V)	UDC o/p (V)	Battery o/p(V)	Battery SOC (%)	BDC o/p (V)	Inverter o/p (V)	Load Position (s)	Inverter/Rectifier Mode
3	8.4	Mode 1	15	11.7	24	24	35	0	0	ON/OFF	Stand-alone
5	13.9	Mode 2	15	11.9	24	24	58	47.6	93.8	ON/OFF	Stand-alone /Grid
7	19.5	Mode 3	15	12.1	24	0	82	47.9	95.1	ON/OFF	Stand-alone /Grid-Inverter
8.65	24.1	Mode 4	0	0	0	24	81	47.6	94	ON/OFF	Stand-alone
11	30.6	Mode 5	0	0	0	23.9	34	48.2	98	ON/OFF	Grid-rectifier



(a) Hard ware setup



(b) wind mill

Figure 9. Real time implementation

5. CONCLUSIONS

The present work is highly focused on five modes of operation in wind energy storage system for an effective operation. The system circuits and components are designed by mathematical modeling which are represented in the form of Eqs. Based on the modeling, the system has been designed in MATLAB/Simulink software, and the recommended controllers are provided for all the converter circuits. All the three parameters and all conditions were defined; based on the parameter conditions, the circuit operates in closed loop by means of main controller. In all the modes of operation, the system's performance in terms of real-time experimentation and simulation is verified. We found a close resemblance between simulation and experimental results. The novelty of this proposed system is its main controller. The main controller operates the whole system in closed loop in an effective way.

REFERENCES

[1] Fujimoto Y, Takahashi Y, Hayashi Y. (2018). Alerting to rare large-scale ramp events in wind power generation. *IEEE Transactions on Sustainable Energy* (99): 1-1. <https://doi.org/10.1109/TSTE.2018.2822807>

[2] Averous NR. (2017). Development of a 4 MW full-size wind-turbine test bench. *IEEE Journal of Emerging and*

Selected Topics in Power Electronics 5(2): 600-609. <https://doi.org/10.1109/JESTPE.2017.2667399>

[3] Chen X, Wang L, Sun H, Chen Y. (2017). Fuzzy logic based adaptive droop control in multi terminal HVDC for wind power integration. *IEEE Transactions on Energy Conversion* 32(3): 1200-1208. <https://doi.org/10.1109/TEC.2017.2697967>

[4] Shi J, Lee WJ, Liu X. (2018). Generation scheduling optimization of wind-energy storage system based on wind power output fluctuation features. *IEEE Transactions on Industry Applications* 54(1): 10-17. <https://doi.org/10.1109/TIA.2017.2754978>

[5] Chen X, Jiang Y, Yu K, Liao Y, Xie J, Wu Q. (2017). Combined time-varying forecast based on the proper scoring approach for wind power generation. *The Journal of Engineering* 2017(14): 2655-2659. <https://doi.org/10.1049/joe.2017.0843>

[6] Pan Y. (2018). Towards the robust small-signal stability region of power systems under perturbations such as uncertain and volatile wind generation. *IEEE Transactions on Power Systems* 33(2): 1790-1799. <https://doi.org/10.1109/TPWRS.2017.2714759>

[7] Chen L, Min Y, Dai Y, Wang M. (2017). Stability mechanism and emergency control of power system with wind power integration. *IET Renewable Power Generation* 11(1): 3-9. <https://doi.org/10.1049/iet-rpg.2016.0147>

[8] Yao J, Yu M, Gao W, Zeng X. (2017). Frequency regulation control strategy for PMSG wind-power generation system with flywheel energy storage unit. *IET Renewable Power Generation* 11(8): 1082-1093. <https://doi.org/10.1049/iet-rpg.2016.0047>

[9] El-Arroudi JG. (2018). Performance of interconnection protection based on distance relaying for wind power distributed generation. *IEEE Transactions on Power Delivery* 33(2): 620-629. <https://doi.org/10.1109/TPWRD.2017.2693292>

[10] Liu YQ, Sun Y, David Infield, Zhao Y, Han S, Yan J. (2017). A hybrid forecasting method for wind power ramp based on Orthogonal Test and Support Vector Machine (OT-SVM). *IEEE Transactions on Sustainable Energy* 8(2). <https://doi.org/10.1109/TSTE.2016.2604852>

[11] Wan YH, Bucaneg D. (2002). Short-term power fluctuations of large wind power plants. *Journal of Solar Energy Engineering* 124-427. <https://doi.org/10.1115/1.1507762>

[12] Kim SJ, Choi WS, Pilawa-Podgurski R, Hanumolu PK. (2018). A 10-MHz 2–800-mA 0.5–1.5-V 90% peak efficiency time-based buck converter with seamless transition between PWM/PFM modes. *IEEE Journal of Solid-State Circuits* 53(3): 814-824. <https://doi.org/10.1109/JSSC.2017.2776298>

[13] Yang WH. (2018). A constant-on-time control DC–DC buck converter with the pseudowave tracking technique for regulation accuracy and load transient enhancement. *IEEE Transactions on Power Electronics* 33(7): 6187-6198. <https://doi.org/10.1109/TPEL.2017.2746659>

[14] Huang YW, Kuo TH, Huang SY, Fang KY. (2018). A four-phase buck converter with capacitor-current-sensor calibration for load-transient-response optimization that reduces undershoot/overshoot and shortens settling time to near their theoretical limits. *IEEE Journal of Solid-*

- State Circuits 53(2): 552-568.
<https://doi.org/10.1109/JSSC.2017.2768412>
- [15] Nien CF. (2017). A novel adaptive quasi-constant on-time current-mode buck converter. *IEEE Transactions on Power Electronics* 32(10): 8124-8133.
<https://doi.org/10.1109/TPEL.2016.2633760>
- [16] Schellekens JM, Huisman H, Duarte JL, Hendrix MAM, Lomonova EA. (2018). An analysis of the highly linear transfer characteristics of dual-buck converters. *IEEE Transactions on Industrial Electronics* 65(6): 4681-4690.
<https://doi.org/10.1109/TIE.2017.2772175>
- [17] Katuri R, Gorantla SR. (2018). Math function based controller applied to electric/hybrid electric vehicle in modelling. *Measurement and Control A* 91(1): 15-21.
https://doi.org/10.18280/mmc_a.910103
- [18] Guo Z, Sun K, Wu TF, Li C. (2018). An improved modulation scheme of current-fed bidirectional DC–DC converters for loss reduction. *IEEE Transactions on Power Electronics* 33(5): 4441-4457.
<https://doi.org/10.1109/TPEL.2017.2719722>
- [19] Babaei E, Saadatizadeh Z, Cecati C. (2017). High step-up high step-down bidirectional DC/DC converter. *IET Power Electronics* 10(12): 1556-1571.
<https://doi.org/10.1049/iet-pel.2016.0977>
- [20] Sri Revathi B, Mahalingam P. (2018). Modular high-gain DC–DC converter for renewable energy micro grids. *Electrical Engineering* 100: 1913-1924.
<https://doi.org/10.1007/s00202-017-0673-5>